GESP-7035
MARCH 1970

SPACE SYSTEMS

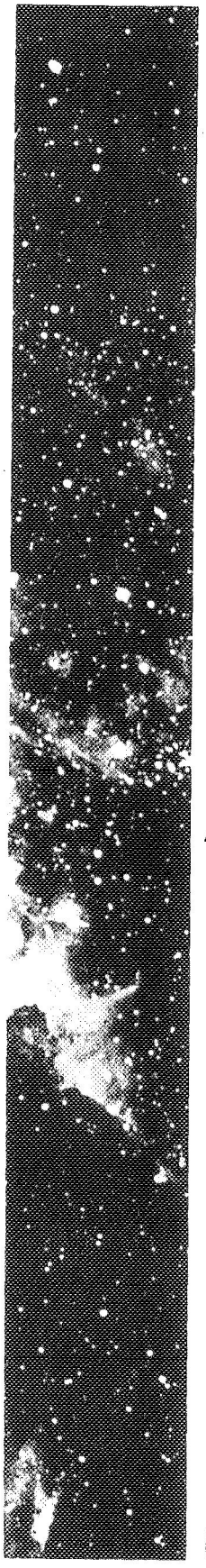

A DESIGN STUDY FOR A MAGNETOHYDRODYNAMIC POWER SYSTEM FOR A NUCLEAR ELECTRIC PROPELLED UNMANNED SPACECRAFT

QUARTERLY REPORT

COVERING THE PERIOD 26 DECEMBER 1969 TO 25 MARCH 1970

PREPARED UNDER CONTRACT JPL 952415

FOR

PROPULSION RESEARCH AND ADVANCED CONCEPTS SECTION
JET PROPULSION LABORATORY
4800 OAK GROVE DRIVE
PASADENA, CALIFORNIA, 91103

GENERAL ELECTRIC

NSP NUCLEAR SYSTEMS PROGRAMS
ISOTOPE POWER SYSTEMS OPERATION

GESP-7035
MARCH 1970

A DESIGN STUDY FOR A MAGNETOHYDRODYNAMIC POWER SYSTEM FOR A NUCLEAR ELECTRIC PROPELLED UNMANNED SPACECRAFT

QUARTERLY REPORT

COVERING THE PERIOD 26 DECEMBER 1969 TO 25 MARCH 1970

PREPARED UNDER CONTRACT JPL 952415

FOR

PROPULSION RESEARCH AND ADVANCED CONCEPTS SECTION
JET PROPULSION LABORATORY
4800 OAK GROVE DRIVE
PASADENA, CALIFORNIA, 91103

THIS WORK WAS PERFORMED FOR THE JET PROPULSION LABORATORY, CALIFORNIA INSTITUTE OF TECHNOLOGY AS SPONSORED BY THE NATIONAL AERONAUTICS AND SPACE ADMINISTRATION UNDER CONTRACT NAS7—100

ISOTOPE POWER SYSTEMS OPERATION
GENERAL ELECTRIC
SPACE DIVISION
KING OF PRUSSIA PARK
P. O. Box 8661 • Philadelphia, Penna. 19101

This report contains information prepared by the General Electric Company under JPL subcontract. Its content is not necessarily endorsed by the Jet Propulsion Laboratory, California Institute of Technology, or the National Aeronautics and Space Space Administration.

ABSTRACT

This report discusses the work performed since the midterm of a one-year design study of a nuclear electric propelled spacecraft using a magnetohydrodynamic (MHD) power system. The parametric variation of shield and structure weight are discussed as well as the effects of decreasing cycle efficiency and increasing temperature. There appears to be no strong advantage to increasing cycle temperature above about 1800^{o}F.

TABLE OF CONTENTS

LIST OF ILLUSTRATIONS

LIST OF TABLES

SECTION 1

INTRODUCTION

On May 26, 1969, the General Electric Company began a design study for the magneto-hydrodynamic (MHD) power system for a nuclear-electric propelled unmanned spacecraft. This work is being performed for the Jet Propulsion Laboratory under contract number JPL 952415, and is based on MHD system technology being developed by the Jet Propulsion Laboratory. The purpose of this study is to provide size, weight and mission performance estimates for nuclear-electric propelled unmanned spacecraft using MHD power systems rated at 100 kWe to 3 MWe. This study is also intended to guide future MHD development by discovering specific requirements associated with spacecraft power system design. The spacecraft design of principal interest is one whose unconditioned power output is a nominal 300 kW(e). The weight goal for this spacecraft is 10,000 pounds including reactor, shielding, MHD conversion equipment, power distribution and conditioning equipment, thruster subsystems, and structure.

The work of this study program is divided into four principal tasks:

1. Task 1 - System Evaluation - The purpose of this task is to establish guidelines and design requirements for the program and to measure the designs generated in the program against these guidelines and requirements.

2. Task 2 - Powerplant Design - The purpose of this task is to provide the engineering analysis and design information necessary for spacecraft design layout. This will include parametric analyses to identify the influence of major plant variables on powerplant and spacecraft characteristics. This task also includes evaluation of the effects of changes in technology levels associated with the powerplant components.

3. Task 3 - Spacecraft Design - The purpose of this task is to define the arrangement, mechanical design and weight estimation for the MHD spacecraft designs.

4. Task 4 - Mission Analysis and Engineering - The purpose of this task is to perform the analysis necessary to evaluate the mission capabilities of the various spacecraft, and to perform a preliminary assessment of prelaunch, launch and flight operations, specifically with respect to aerospace nuclear safety.

In the first half of this one-year study a baseline design spacecraft and powerplant were developed. This baseline design is a 300 kWe system and assumes reasonable extension of component technology based on current test work. In the second half of the year the space-

craft and the powerplant design are being varied parametrically to evaluate the effects of changes in output power level and operating parameters, and to evaluate the effects of improvements in the technology of key components. At the end of the year-long Phase I, a reference MHD spacecraft design will be selected.

The MHD spacecraft study is being performed concurrently with a design study of a thermionic reactor power system for nuclear-electric propelled unmanned spacecraft, (JPL Contract No. 952381). Wherever possible, design bases for the MHD spacecraft are being made the same as those for the thermionic spacecraft in order to provide a clear comparison of these two power systems. In particular, the MHD spacecraft baseline design is using the same payload thruster subsystem and mission profile as the Phase I thermionic reactor spacecraft.

The MHD spacecraft study is proceeding on schedule. The computer programs for MHD generator and cycle analysis have been received from JPL and converted to basic FORTRAN IV for use on the IBM 1130 computer. Preliminary startup and reactor characterization have been completed. Configuration tradeoffs were made to select the most efficient overall spacecraft configuration for development of the baseline spacecraft design. The computer programs were combined into a single MHD system program with added models to calculate key variable weights. The MHD System program was used to generate parametric data and the baseline design parameters were thereby selected. The baseline design has been drawn up and its weight calculated.

The Midterm briefing was held on February 10, 1970 and, after a review of the baseline design, direction of the second half work effort was agreed upon. Parametric evaluation of different cycle temperatures, efficiencies and power levels has begun.

SECTION 2
TECHNICAL DISCUSSION

In order to proceed with the parametric evaluation of different MHD cycle temperatures and power levels, it is necessary to provide parametric input data for variation of system components. The combined computer program contains models which calculate MHD generator weight variation and radiator weight variation on an area basis. Still needed are parametric data on other components such as the reactor, the radiation shield, and the support structure. Parametric data for the reactor has already been generated and is reported in References 1 and 2; this report presents parametric data for the radiation shield and the support structure. In addition, the first results for variation of velocity factor and temperature level are discussed.

2.1 MHD REACTOR SHIELD PARAMETRIC STUDY

2.1.1 INTRODUCTION

Using the results of a fast reactor shield calculation reported in Reference 3, estimates were made of the shielding requirements for the MHD reactor as a function of reactor power level and shield/payload separation distance.

2.1.2 ANALYTICAL MODEL

The separation distances considered here, 40 feet or greater, permit the simplifying assumption that the dose rate varies as the inverse square of the distance from the shield. This approximation will hold quite well for separation distances greater than about twice the diameter of the shield face, which in the present case would be about eight feet. It is also assumed that the dose rate will be directly proportional to the power level. This would be strictly true if the reactor geometry were to be fixed and increase in power were effected by an increase in the power density. It would be an over estimate of the dose rate if the power increase was brought about by maintaining the power density and increasing the core volume through an increase in its length. The added source volume in this case would be shielded in part by the original core volume and hence its contribution to the dose

rate would be reduced. If the core volume were increased by increasing the core diameter, the contribution of the added source to the dose rate would be somewhere between the two cases discussed above.

In order to minimize the dose rate at the payload due to radiation scattered from the radiator or other strucutres, the radiator and the equipment located directly behind the shield are to be within the shielded cone. This requirement results in a shield whose lateral extension is essentially unaffected by the variation in the shield/payload separation distance considered here. Hence, the rear shield face, viewed as a surface source of radiation, will have a constant area.

The variation of the neutron flux with the thickness of the LiH shield is based upon the results of a calculation of fission spectrum neutrons in an infinite medium of LiH.

The variation of the gamma dose with the thickness of the LiH shield is based upon the results of a shield calculation performed at Oak Ridge National Laboratory for the Unmanned Thermionic Spacecraft Study (Reference 4).

2.1.3 RESULTS

The neutron and gamma ray dose limits at the payload, for 1.4×10^4 equivalent full power operating hours, were set at 10^{12} nvt for neutrons with energies above 1 Mev, and 10^7 rads for gamma rays. It was found that the LiH shield required for the neutrons was more than adequate for the gamma rays.

The LiH shield axial thickness as a function of reactor power level and shield/payload separation distance is given in Figure 1.

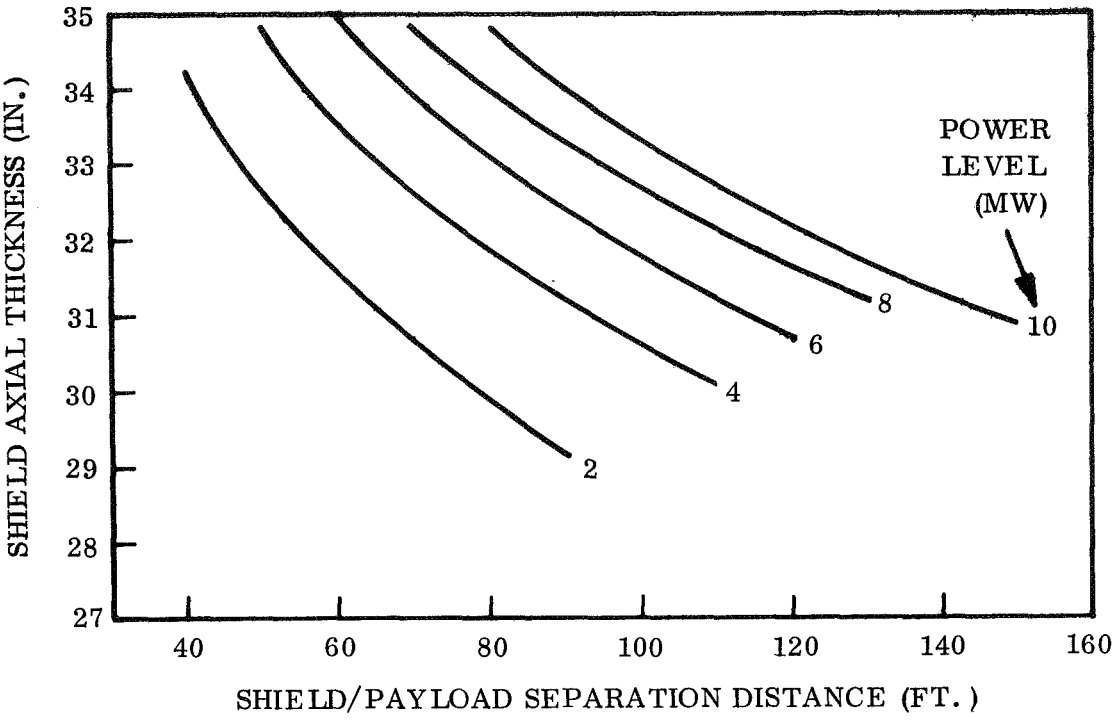

Figure 1. Variation of Radiation Shield Thickness With Reactor Power Level and Payload Separation Distance

2.2 MHD SPACECRAFT RADIATOR SUPPORT STRUCTURE

2.2.1 INTRODUCTION

The purpose of this study is to determine the effects of the weight of the reactor and the length of the main radiator on the weight of the support structure for the main radiator bay.

This study is an extension of the work reported previously in Reference 2; however, it is limited to a modified version of Configuration 4, which has been selected as the baseline design. The baseline design, shown schematically in Figure 2, utilizes a triform geometry for the main radiator. The thermally configured main radiator requires additional structure to support the loads induced during launch. The limiting load conditions considered, represent combined static and dynamic loads for a Titan IIIC7 launch vehicle and are shown below:

Stage I burnout - 3 g's lateral and 6 g's axial

Stage II burnout - 0.67 g's lateral and 4 g's axial

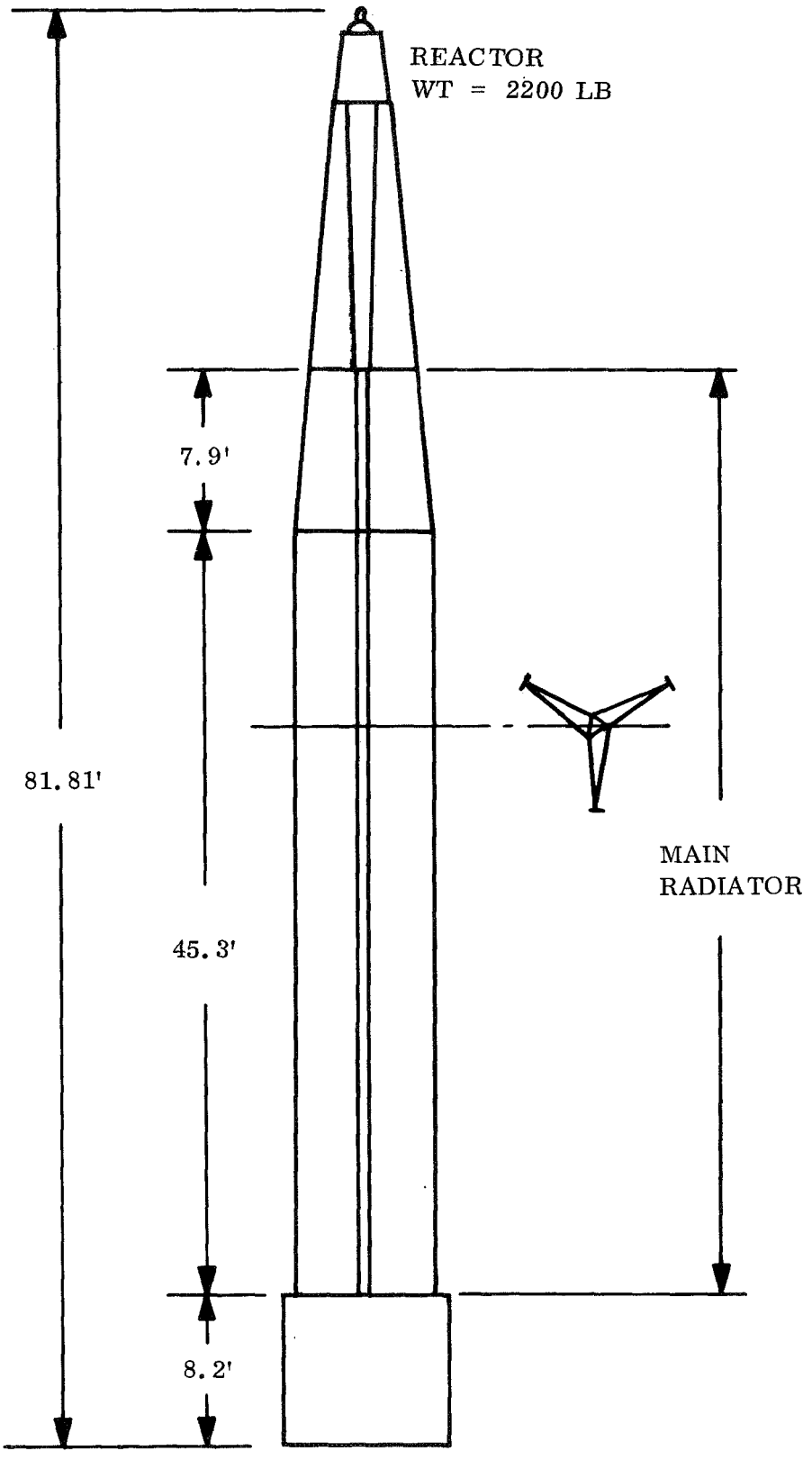

Figure 2. Baseline Design

2.2.2 SUMMARY

The weights of the structures which must be added to the main radiator bay to support the launch loads are presented in Figures 3 and 4.

Figure 3 shows the weight of the required nondisposable structure as a function of the length of the main radiator and the weight of the reactor. This structure consists of longitudinal support members permanently attached to the outer edge of each of the three radiator panels. These members are formed from 0.06-inch thick sheet of 301 Stainless Steel in the half hard condition and are sized to support the loads associated with the Stage II burnout condition. Included in the weight is a seven percent factor for fittings.

Figure 4 shows the weight of the required disposable structure as a function of the length of the main radiator and the weight of the reactor. The disposable structure consists of longitudinal support members pinned to the outer edges of each of the three radiator panels, joined by diagonal tension members to provide lateral and torsional stability. The longitudinal members are channel sections and the diagonal tension members are thin wall cylindrical tubes, both formed from 301 SS in the half hard condition. The disposable structure members are sized to provide the additional strength necessary to support the loads associated with the Stage I burnout condition. Following Stage I burnout, they are ejected, reducing the weight of the spacecraft. Included in the weight is a 15 percent factor for fittings.

Design details for the support structure are described in References 1 and 2.

2.2.3 CONCLUSIONS

Since the support structures have been sized for strength, without regard to lateral excursions of the tip or the frequency of the fundamental bending mode of vibration, the following studies are recommended if the longer spacecraft show promise from other considerations:

1. The maximum lateral deflection of the tip of the spacecraft should be calculated to determine if the dynamic envelope of the shroud is violated.

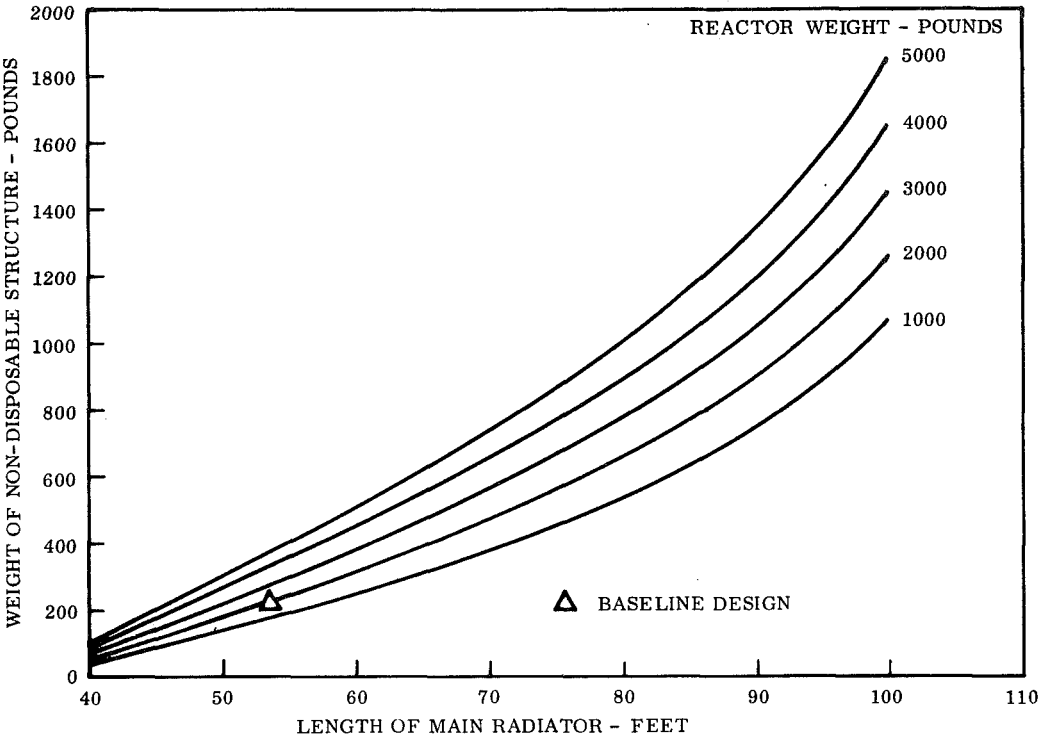

Figure 3. MHD Spacecraft Main Radiator Weight of Nondisposable Support Structure vs. Length of Radiator and Reactor Weight

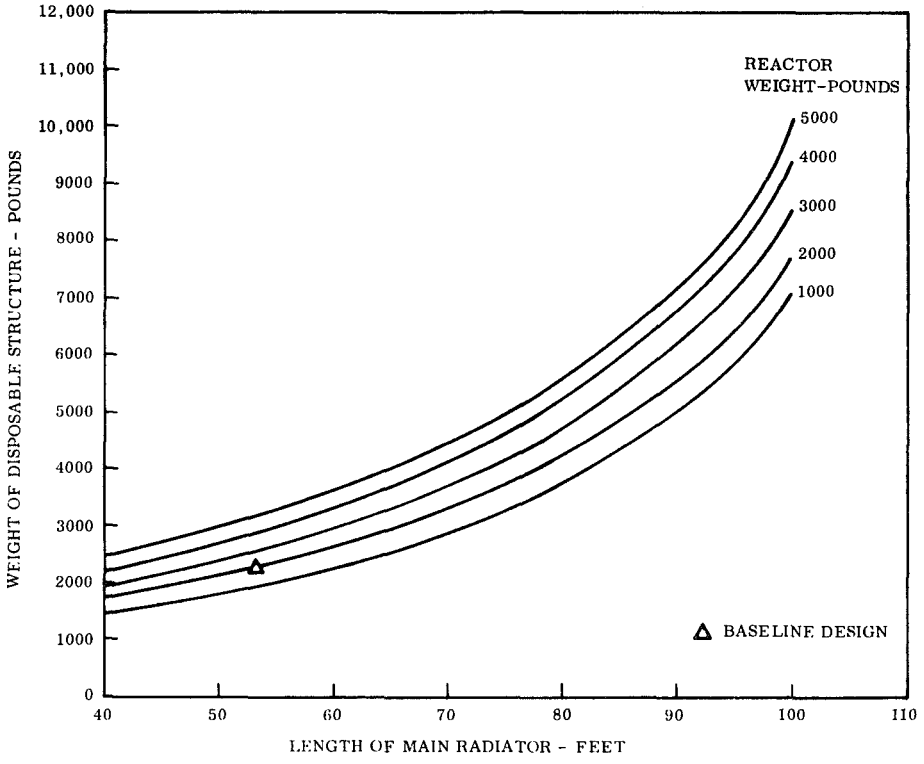

Figure 4. MHD Spacecraft Main Radiator Weight of Disposable Support Structure vs. Length of Radiator and Reactor Weight

2. The fundamental frequency of the spacecraft in the lateral direction should be calculated to determine if it is low enough to cause severe coupling between the launch vehicle control system and the launch system structural dynamics.

Either of these considerations could require a significant increase in the weight of the support structure for the longer spacecraft.

2.3 VELOCITY FACTOR EFFECTS

2.3.1 VELOCITY FACTOR DEFINITION

In the MHD cycle and generator calculations a velocity factor, K_v, is used as a multiplier on the generator inlet velocity; K_v is discussed in Appendix II of Reference 1. This velocity factor is a user input which can account for non-ideal behavior of the lithium/cesium separator. In the baseline design the factor was taken as 1.0, representing ideal separator performance. Friction losses in the separator can be reflected by a decreasing K_v; in that sense K_v x 100 may be considered separator efficiency. From an analytical standpoint K_v can be greater than one if it is used to represent two other fluid mechanisms as well as friction loss. The calculation of the generator inlet velocity involves an assessment of vapor/liquid slip in the two-phase nozzles and calculation of the amount of cesium dissolved in the lithium stream. If one desires to be less conservative in these two respects than the baseline design, a velocity factor of greater than one is a convenient analytical tool to do so.

2.3.2 VELOCITY FACTOR CALCULATIONS

A set of runs were made with Run No. 19 (the baseline design) as the standard and the velocity factor varied from the baseline value of 1.0 down to 0.8; Table 1 lists the runs. Generator and system quantities normalized by the values calculated in Run 19 are shown in Figure 5 as a function of velocity factor. Decreased velocity factor causes decreased system efficiency with the resultant increase in primary radiator size, coil loss and reactor weight. Secondary radiator temperatures are low so the calculated areas are large or in some runs the radiator temperature is below the sink temperature. For this reason, coil loss is given as more meaningful information than secondary radiator area.

Table 1. Runs with Velocity Factor Varied

Run No.	Vel. Factor K_V	Nozzle Area Ratio	Gamma Coil Ratio γ	ΔP Sep. to Cond. (N/M^2)	Inlet Field (Wb/M^2)
19	1.0	3.25	0.9	0.15×10^5	0.47
20	0.95				
21	0.9				
22	0.85				
23	0.8				
24	0.85	3.5			
25		3.75			
26		3.25		0.2×10^5	
27				0.15×10^5	0.49
28					0.45
29			1.0		0.47

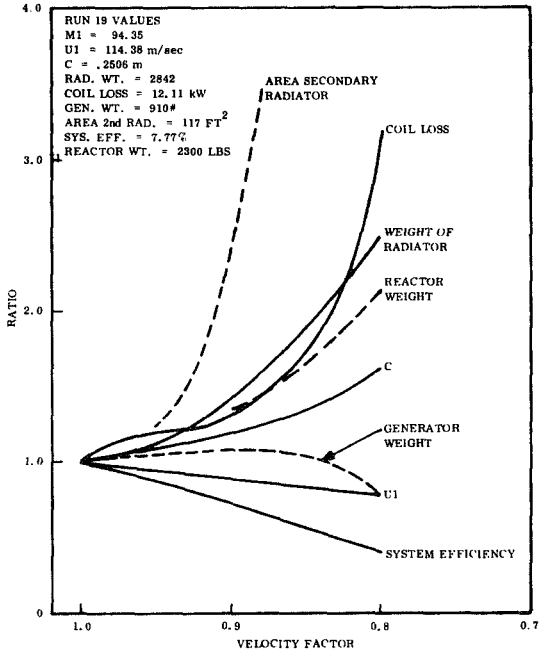

Figure 5. Effect of Velocity Factor Variation

The velocity factor = 0.85 case, Run 22, was investigated in Runs 23 to 29 for sensitivity to various parameters to check the possibility for optimization. The parameter variations are given in Table 1 and results are given in Table 2. Increasing area ratio, Run 25, produced the most favorable results but could not increase efficiency appreciably.

Table 2. Effect of Velocity Factor

Run No.	Efficiency %	Generator Weight lbs	Primary Rad. Weight lbs	Coil Loss kW
22	4.4	946	5202	21.12
24	4.57	957	5257	19.05
25	4.74	966	5358	17.40
26	4.39	946	5419	21.12
27	4.31	647	5311	30.34
28	4.44	1341	5147	15.02
29	4.38	859	5217	22.09

2.3.3 CONCLUSIONS

As can be seen in Figure 5, only the secondary (coil cooling) radiator area gets out of hand in the range of velocity factor from 1.0 to 0.9. This is not a severe problem since manual reoptimization of coil loss, coil ratio, coil temperature, and radiator fin efficiency can produce an acceptably low radiator area. This is, in fact, what is done to translate a computer generated MHD spacecraft design to a detailed layout.

The detailed assessment of the effects of efficiency variation on total system weight is still in progress but an estimate was made by breaking out the reactor and radiator weight from the baseline design powerplant weight of 15,810 pounds to leave a weight of approximately 11,000 pounds for the rest of the powerplant. These other portions of the powerplant will not suffer any notable weight increase as will the reactor and main radiator. Figure 6 illustrates the change in powerplant weight with decreasing system efficiency based on a normalization to the baseline design system. Note that reducing the system efficiency by a factor of two increases powerplant weight by about one-third.

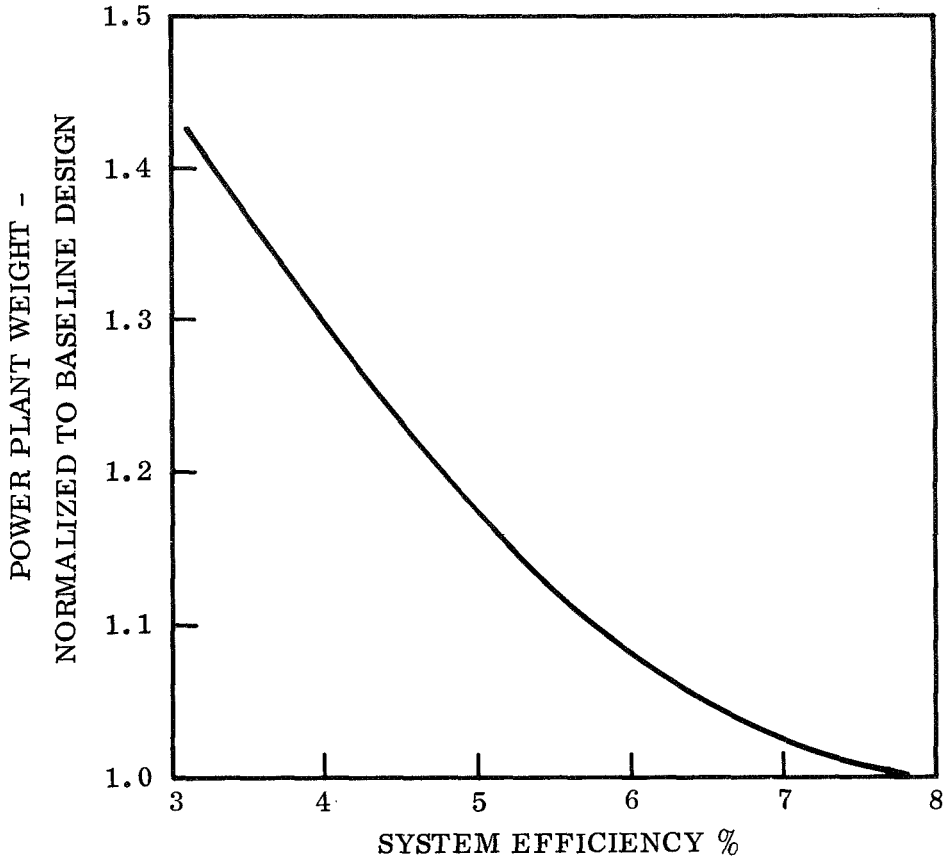

Figure 6. Variation of Powerplant Weight With System Efficiency

2.4 EFFECTS OF SYSTEM TEMPERATURE LEVEL

2.4.1 INTRODUCTION

The lithium/cesium MHD cycle used in this study does not respond to system temperature change in the same way as typical Rankine cycle systems. As system temperature increases, the heat rejection temperature can be increased, thereby reducing radiator size and weight. However, offsetting this advantage, the increased temperature will cause more cesium to dissolve in the lithium stream requiring the use of proportionately more cesium; the cycle calculations assume equilibrium solution of cesium in lithium for conservatism.

2.4.2 CALCULATIONS

The next effort was directed toward determining the effect of different temperature levels. Runs 30 to 43 studied the effects of temperature and lithium to cesium mass ratio. Parameters and results are given in Table 3 and the results are also shown in Figures 7 and 8.

Table 3. Effect of Temperature and Li/Cs Ratio

Run No.	Temperature °F	Li/Cs Ratio	System Efficiency %	Generator Weight lb	Reactor Weight lb	Primary Radiator Weight lb	Secondary Radiator Weight lb	Total
19	1800	14	7.77	910	2300	2842	12	6064
30	1800	11	7.65	916	2500	2876	93	6385
31	1850	14	7.56	1003	2600	2638	79	6320
32	1850	11	7.61	1103	2700	2611	46	6460
34	1900	14	7.19	1036	2900	2505	63	6504
35	1900	11	5.97	1328	2800	2402	32	6562
36	1900	8	7.17	1022	2900	2520	35	6477
37	1900	5	5.97	519	3500	3098	274	7391
38	1950	14	6.51	930	3600	2503	75	7108
39	1950	11	7.14	1206	3300	2276	34	6816
40	1950	8	7.11	1386	3300	2300	23	7009
41	2000	11	6.56	1182	4150	2239	36	7607
42	2000	8	6.9	1848	3900	2144	19	7911
43	2000	5	6.06	974	4430	2504	25	7933

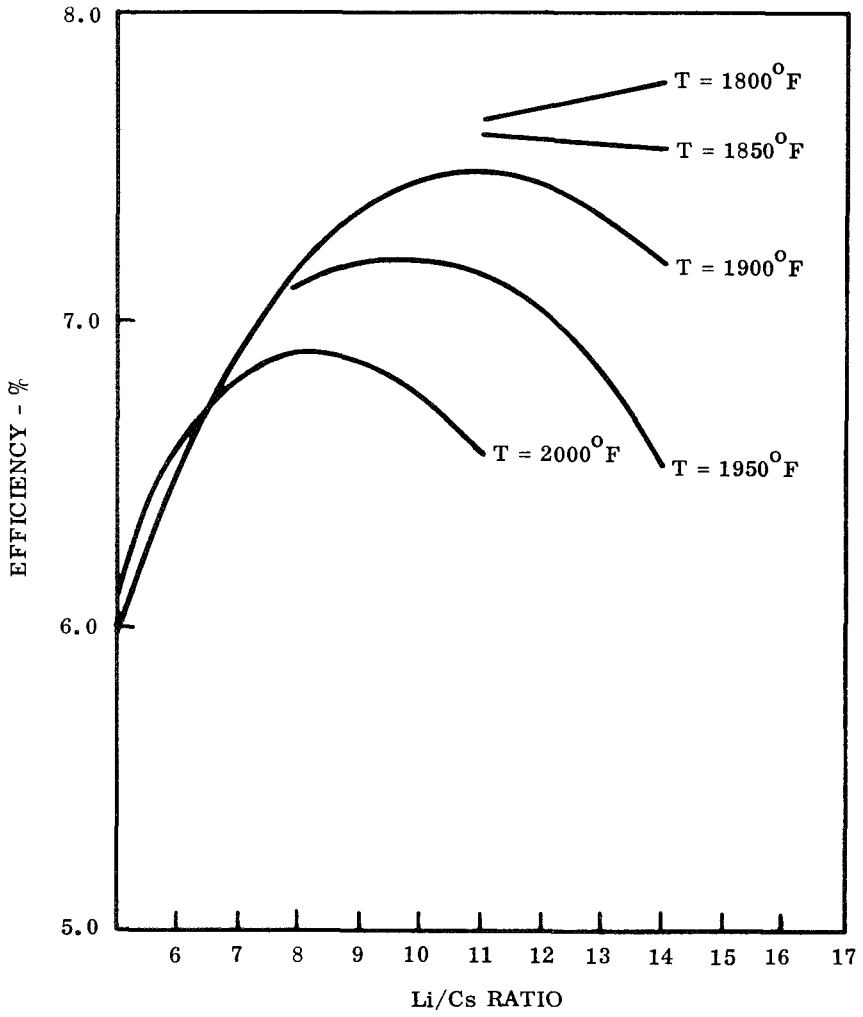

Figure 7. Effect of Temperature and Li/Cs Mass Ration on Efficiency

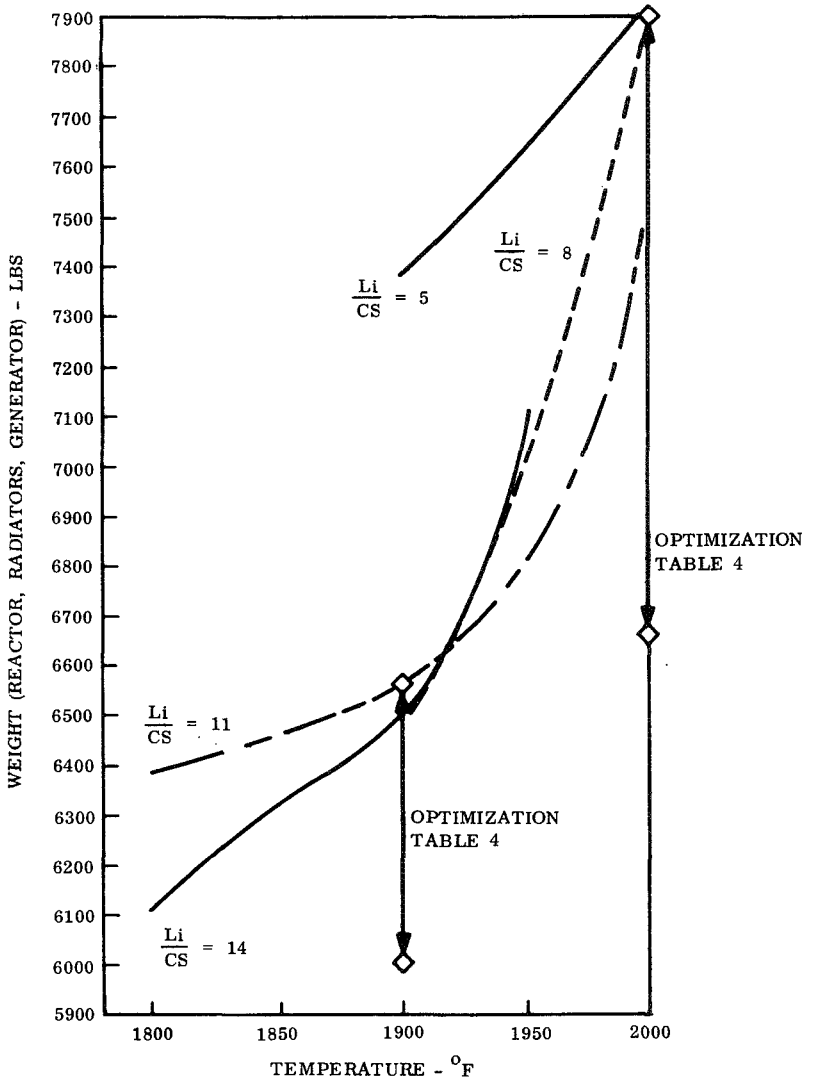

Figure 8. Effect of Temperature and Li/Cs Mass Ratio on Weight

It can be seen from Figure 7 that increased temperature causes the maximum efficiency condition to occur at a lower lithium/cesium (Li/Cs) mass ratio with a reduction in the efficiency. A parameter more important than efficiency for spacecraft studies is weight. Figure 8 shows the sum of reactor, generator, primary and secondary radiator weight. There is very little spread due to Li/Cs ratio between 8 and 14 but weight increases significantly with temperature level. This is due mostly to reactor weight although in some of the runs, the generator weight is also high.

The only variable except temperature in these results is lithium to cesium mass ratio and the system is not optimum as indicated by the generator weights. A series of runs were made to optimize the cases Li/Cs = 11, T = 1900^{o}F and Li/Cs = 8, T = 2000^{o}F with Runs No. 35 and 42 as the baselines respectively. The variables are given in Table 4.

Table 4. Runs for Optimization at 1900^{o}F and 2000^{o}F

Run No.	Case		Nozzle Area Ratio	Inlet Field Wb/M^2	N Upstream Vanes	N Downstream Vanes
	Li/Cs Ratio	T ^{o}F				
35	11	1900	3.25	0.47	18	28
44	11	1900	3.0	0.47	18	28
45	11	1900	3.5	0.47	18	28
46	11	1900	3.25	0.45	18	28
47	11	1900	3.25	0.49	18	28
48	11	1900	3.25	0.47	22	34
49	11	1900	3.25	0.47	14	22
50	11	1900	3.25	0.49	22	34
42	8	2000	32.5	0.47	22	34
51	8	2000	3.25	0.49	22	34
52	8	2000	3.25	0.51	22	34
53	8	2000	3.25	0.53	22	34

Considering the Li/Cs = 11, T = 1900^{o}F case first, Figure 9 shows little variation in system efficiency, therefore, reactor weight is constant. The optimum generator design (from a weight viewpoint) has a higher inlet field, near 0.49, compared to results at 1800^{o}F. Comparing Run 47 to Run 35, the generator weight is reduced more than the increase in secondary radiator

weight increase. Higher fields produce large secondary radiator weight or the need for secondary radiator temperature lower than sink temperature.

The Li/Cs = 8, T = 2000°F case is optimized with inlet field only. Results are shown in Figure 10 illustrating optimization at higher inlet field as temperature is increased.

Weights from optimized runs; Run 19 for T = 1800°F, Run 47 for T = 1900°F, and Run 52 for T = 2000°F are shown in Figure 8. From a system weight viewpoint there is no incentive to go to the higher temperature levels. This conclusion is re-enforced when one considers unaccounted for weight increases in piping, nozzles, etc., at high temperature levels. Results shown in Figures 9 and 10 are also given in Table 5.

Table 5. Weights for Optimization at 1900°F and 2000°F

Run No.	Generator Weight Pounds	Primary Radiator Weight Pounds	Secondary Radiator Weight Pounds	Reactor Weight Pounds	Total
35	1328	2402	32	2800	6562
44	1365	2338	34	2800	6537
45	1292	2476	30	2800	6598
46	2706	2419	18	2800	7943
47	652	2403	145	2800	6000
48	1062	2429	43	2800	6334
49	1327	2406	32	2800	6565
50	656	2422	140	2800	6018
42	1848	2144	19	3900	7911
51	920	2139	34	3900	6993
52	546	2126	85	3900	6657
53	308	2138	*	3900	----

*Radiator temperature below sink temperature

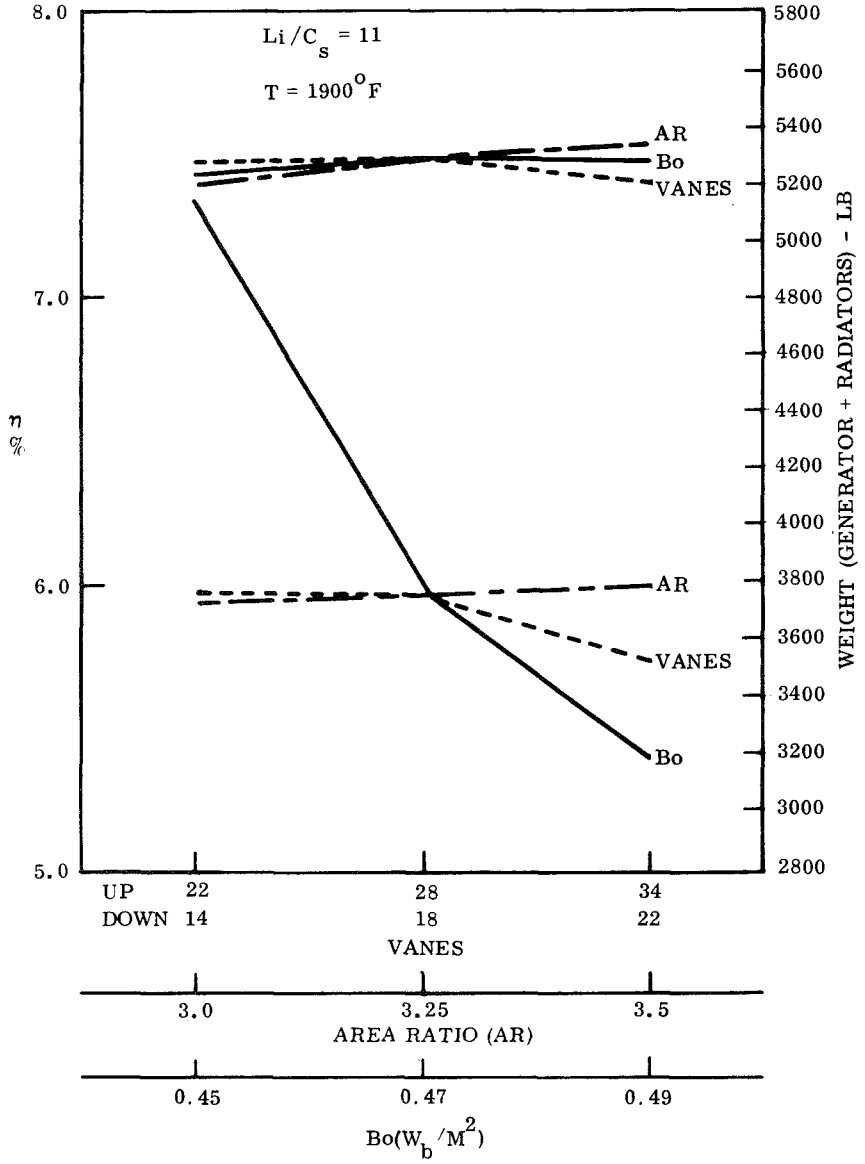

Figure 9. Optimization of Case 11 (Run 35)

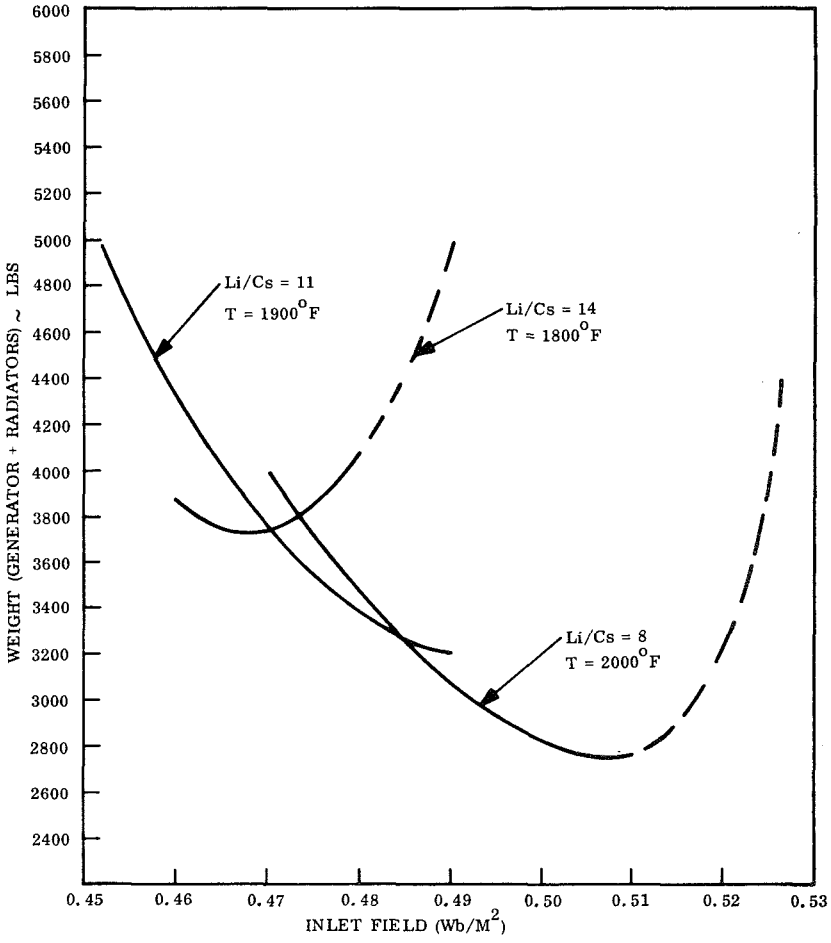

Figure 10. Effect of Inlet Field on Weight

SECTION 3

CONCLUSIONS

From review of the work reported in this report the following conclusions are drawn:

1. System weight is not directly proportional to system efficiency; weight increases with reduced efficiency are chiefly in reactor and radiator weight.

2. There is no incentive to increase MHD cycle temperature above $1800^{o}F$.

SECTION 4

RECOMMENDATIONS

1. Continue the evaluation of system weight variation with reduced efficiency looking specifically at other component weights which may also change (shield, piping, structure).

2. Use the 1800^{o}F cycle temperature for evaluation of different power levels.

SECTION 5

TECHNOLOGY

No new technology items have been identified.

SECTION 6

REFERENCES

1. GESP-7017, A Design Study for a Magnetohydrodynamic Power System for a Nuclear Electric Propelled Unmanned Spacecraft. Quarterly Progress Report Number 1, September 1969.

2. GESP-7025, A Design Study for a Magnetohydrodynamic Power System for a Nuclear Electric Propelled Unmanned Spacecraft, Midterm Report, December 1969.

3. PWAC-445, Preliminary Design of the 2 MWT Reactor and Shield (PWAR-20) for the SNAP-50/SPUR Powerplant, December 30, 1964.

4. Letter from F. R. Mynatt (ORNL) to W. Z. Prickett (GE) dated September 23, 1969.